Intelligent Reflecting Surface-Assisted Adaptive Beamforming for Blind Interference Suppression

Peilan Wang, Jun Fang, *Senior Member, IEEE*, Bin Wang, and Hongbin Li, *Fellow, IEEE*

***Abstract*—In this paper, we consider the problem of adaptive beamforming (ABF) for intelligent reflecting surface (IRS)-assisted systems, where a single antenna receiver, aided by a close-by IRS, tries to decode signals from a legitimate transmitter in the presence of multiple unknown interference signals. Such a problem is formulated as an ABF problem with the objective of minimizing the average received signal power subject to certain constraints. Unlike canonical ABF in array signal processing, we do not have direct access to the covariance matrix that is needed for solving the ABF problem. Instead, for our problem, we only have some quadratic compressive measurements of the covariance matrix. To address this challenge, we propose a sample-efficient method that directly solves the ABF problem without explicitly inferring the covariance matrix. Compared with the methods which explicitly recover the covariance matrix from its quadratic compressive measurements, our proposed method achieves a substantial improvement in terms of sample efficiency. Simulation results show that our method, using a small number of measurements, can effectively nullify the interference signals and enhance the signal-to-interference-plus-noise ratio (SINR).**

***Index Terms*—Intelligent reflecting surface (IRS), adaptive beamforming, interference cancellation.**

I. Introduction

In recent years, intelligent reflecting surface (IRS), a.k.a., reconfigurable intelligent surface (RIS), has emerged as a revolutionary technology for future wireless communications [1]–[7], owing to its capability in reshaping the wireless propagation environment. Generally, an IRS comprises of a massive number of reflecting elements, each capable of independently introducing a controllable amplitude and phase shift to the impinging signal [8]. By intelligently adjusting the reflection coefficients of the IRS, a smart propagation environment can be created for various purposes, such as boosting system capacity [9], [10], mitigating user interference [2], enhancing physical layer security [11], [12], among others.

Most existing studies require accurate channel state information (CSI) for jointly optimizing the transceiver and the IRS's reflection coefficients. Nonetheless, CSI acquisition for IRS-assisted systems remains a significant challenge in practice [13]–[18]. The reasons for this are as follows. Firstly, the IRS is usually a passive device that cannot transmit or receive signals and is incapable of signal processing. Secondly, the number of channel parameters increases linearly with the number of reflection elements, entailing a substantial amount of training overhead. Thirdly, full CSI acquisition often incurs a high computational complexity due to the need of matrix inversion. Last but not least, in some applications involving non-cooperative sources, it is almost impossible to acquire the CSI associated with these non-cooperative signals.

Recently, some efforts have been made to address the CSI acquisition challenge by leveraging blind beamforming techniques that do not require CSI [19]–[23]. Specifically, [19] proposed an approach that determines the ON/OFF states of each reflecting element based on the conditional sample mean (CSM) of the received signal power. This method was further refined and analyzed for scenarios where the IRS employs discrete phase shifters [20], and extended to systems involving multiple IRSs [21]. The CSM method was shown to achieve the well-known quadratic power scaling law even without full CSI. However, achieving such a gain requires a sample complexity of $\mathcal{O}(L^2(\log L)^3)$, where L is the number of reflecting elements. This high sample complexity poses a significant implementation challenge, particularly when channels vary rapidly or the number of reflecting elements is large. To address this issue, [22] proposed to maximize the long-term channel power for fast-fading channels. On the other hand, [23] found that the CSM method can be interpreted as the ϵ-greedy algorithm used to solve the multi-armed bandit problem in reinforcement learning, and proposed a gradient bandit method to enhance the efficiency of blind beamforming.

In contrast to existing works that primarily focused on enhancing the received signal power, this paper is concerned with the problem of suppressing unknown interference signals with the aid of the IRS. To this end, we propose to minimize the average received signal power, subject to a constraint placed on the desired signal's received power. The formulated problem has a form similar to canonical ABF in array signal processing. Nevertheless, an important distinction between our IRS-assisted ABF problem and the traditional ABF problem is that our problem cannot directly obtain the signal-plus-interference covariance matrix that is needed for ABF. Instead, we only have access to some quadratic compressive measurements of the covariance matrix. Recovering the covariance matrix from its quadratic compressive measurements, a problem known as "covariance sketching"

Peilan Wang, Jun Fang and Bin Wang are with National Key Laboratory of Wireless Communications, University of Electronic Science and Technology of China, Chengdu 611731, China. Bin Wang is also with the Guangdong Dejiu New Energy Co., Ltd, Foshan 528200, China. (Emails: peilan_wangle@uestc.edu.cn, JunFang@uestc.edu.cn)

Hongbin Li is with the Department of Electrical and Computer Engineering, Stevens Institute of Technology, Hoboken, NJ 07030, USA, E-mail: Hongbin.Li@stevens.edu

The work of P. Wang was supported in part by Sichuan Provincial Natural Science Foundation under Grant 2025ZNSFSC1431, the China Postdoctoral Science Foundation under Grants 2024M750357 and GZB20240121. The work of J. Fang was supported in part by the National Key Laboratory of Wireless Communications Foundation under Grants IFN20230205 and IFN202409. The work of H. Li was supported in part by the National Science Foundation under grants CCF-2316865, ECCS-2212940, and ECCS-2332534.

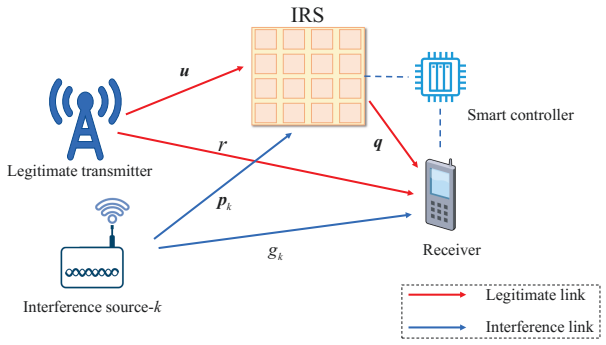

Fig. 1. Illustration of the considered IRS-assisted wireless communication system.

[24]–[26], is sample-costly. Specifically, it was reported in [26] that the number of measurements should exceed the order of $O((L+1)(K+1)^4)$ to recover the covariance matrix with theoretical guarantees, where L denotes the number of reflection elements and K is the number of interference signals. Such a sample complexity becomes problematic in rapidly-changing channel environments. To address this issue, we propose an analytical sample-efficient solution that can automatically nullify the interference signals using only $(K+2)^2$ measurements. This significant sample complexity reduction makes the proposed algorithm more suitable for fast-changing propagation environments.

Specifically, the contributions of this work are summarized as follows:

- The formulation presented in this work is new and has not been reported before. To the best of our knowledge, this is the first work to formulate IRS-assisted blind interference cancellation as an ABF problem. We also clarify the key distinctions between our formulated ABF problem and the canonical one.
- We propose a novel analytical method to solve the formulated ABF problem without the need to explicitly infer the knowledge of the covariance matrix, which is needed for the canonical ABF. Compared with methods that first reconstruct the covariance matrix and then solve the ABF problem, our approach achieves a significant improvement in terms of sample complexity.

The rest of the paper is organized as follows. Section II describes the system model and problem formulation. The proposed analytical solution is introduced and analyzed in Section III, and subsequently extended to fully passive IRS in Section IV. Simulation results are presented in Section V, followed by concluding remarks in Section VI.

II. System Model

A. Signal Model

As illustrated in Fig. 1, we consider an IRS-assisted point-to-point wireless communication system, where a single antenna receiver, aided by an IRS, tries to decode signals from a legitimate transmitter in the presence of multiple (say, K) unknown strong interference signals. The basic idea is that the receiver, based on its received signal samples, adaptively adjusts the IRS's reflection coefficients such that the unknown interference signals are canceled at the receiver whereas the desired signal can be well preserved. Such an idea is reminiscent of the well-known ABF technique in array signal processing, and therefore we refer to the proposed technique developed in this work as "IRS-assisted ABF".

We have the following assumptions concerning the legitimate signal and the interference signals:

- A1 The legitimate signal and interference signals are uncorrelated with each other.
- A2 The legitimate signal and interference signals are assumed to be zero-mean and wide-sense stationary.

Assumption A1 is commonly used in ABF and usually holds valid as the legitimate transmitted signal and the interference signals are from independent sources. Assumption A2 is a widely adopted assumption and usually satisfied in practice as communication signals are known to be cyclostationary and can be treated as stationary over a short time interval.

Suppose the IRS consists of L reflecting elements. Each element on the IRS behaves like a single physical point which combines all the received signals and then re-scatters the combined signal with a certain amplitude and phase shift. Specifically, let θ_l and $\beta_l \leq 1, \forall l$ respectively denote the phase shift and amplitude associated with the lth reflecting element of the IRS. Note that here we assume that the phase shift and the reflection amplitude can be individually controlled. In fact, recent efforts have led to breakthroughs in designing reconfigurable metasurfaces that can simultaneously manipulate both the reflection amplitude and the phase, e.g. [27]. Also, we define the following notations:

- Let $r \in \mathbb{C}$ denote the direct-link channel between the legitimate transmitter and the receiver, and $g_k \in \mathbb{C}$ denote the direct-link channel between the kth interference source and the receiver.
- Let $\boldsymbol{u} \in \mathbb{C}^L$ denote the channel between the legitimate transmitter and the IRS, and $\boldsymbol{p}_k \in \mathbb{C}^L$ denote the channel between the kth interference source and the IRS.
- Let $\boldsymbol{q} \in \mathbb{C}^L$ denote the channel between the IRS and the receiver.

With the above notations, the received signal at the receiver can be written as

$$\begin{aligned} y(t) = & \underbrace{(r+\boldsymbol{q}^H\boldsymbol{\Theta}\boldsymbol{u})s(t)}_{\text{desired signal}} + \underbrace{\sum_{k=1}^{K}(g_k+\boldsymbol{q}^H\boldsymbol{\Theta}\boldsymbol{p}_k)j_k(t)}_{\text{interference signals}} + \underbrace{\epsilon(t)}_{\text{noise}}, \\ \overset{(a)}{=} & \boldsymbol{a}^H\boldsymbol{h}_0 s(t) + \sum_{k=1}^{K}\boldsymbol{a}^H\boldsymbol{h}_k j_k(t) + \epsilon(t) \end{aligned} \tag{1}$$

where $s(t) \sim \mathcal{CN}(0,1)$ and $j_k(t) \sim \mathcal{CN}(0,\sigma_k^2)$ respectively represent the signal of interest (SOI) and the kth interference signal,[1] $\boldsymbol{\Theta} \triangleq \text{diag}(\beta_1 e^{j\theta_1}, \ldots, \beta_L e^{j\theta_L})$ is the reflection matrix

[1]Here, without loss of generality, the signal power is fixed at 1, and σ_k^2 represents the power of the kth interference source.

of the IRS, and $\epsilon(t) \sim \mathcal{CN}(0, \sigma_w^2)$ is the additive Gaussian noise; in (a), we have

$$r + \boldsymbol{q}^H \boldsymbol{\Theta} \boldsymbol{u} = \underbrace{[1 \;\; \boldsymbol{v}^H]}_{\boldsymbol{a}^H} \underbrace{\begin{bmatrix} r \\ \boldsymbol{q}^* \odot \boldsymbol{u} \end{bmatrix}}_{\boldsymbol{h}_0} = \boldsymbol{a}^H \boldsymbol{h}_0, \tag{2}$$

$$g_k + \boldsymbol{q}^H \boldsymbol{\Theta} \boldsymbol{p}_k = [1 \;\; \boldsymbol{v}^H] \underbrace{\begin{bmatrix} g_k \\ \boldsymbol{q}^* \odot \boldsymbol{p}_k \end{bmatrix}}_{\boldsymbol{h}_k} = \boldsymbol{a}^H \boldsymbol{h}_k, \tag{3}$$

with $\boldsymbol{v} \triangleq [\beta_1 e^{j\theta_1} \;\; \ldots \;\; \beta_L e^{j\theta_L}]^H$ denoting the reflection vector, $\odot$ denoting the Hadamard product and $\boldsymbol{a} \triangleq [1 \;\; \boldsymbol{v}^H]^H$ denoting the *augmented reflection vector* with its first entry equal to one. We also have the following assumptions regarding the cascaded channels $\{\boldsymbol{h}_k \in \mathbb{C}^{(L+1)}\}_{k=0}^K$:

- A3 The cascaded channels $\{\boldsymbol{h}_k\}_{k=0}^K$ between the legitimate transmitter/the interfering sources and the receiver are assumed to be linearly independent.
- A4 The cascaded channel between the legitimate transmitter and the receiver, i.e., $\boldsymbol{h}_0 \in \mathbb{C}^{(L+1)}$, is assumed to be known *a priori*, whereas the cascaded interference channels $\{\boldsymbol{h}_k\}_{k=1}^K$ are unknown.

Assumption A3 is generally satisfied when signal sources are spatially separated. In Assumption A4, we assume the cascaded communication channel $\boldsymbol{h}_0$ is known *a priori*. In practice, the legitimate channel $\boldsymbol{h}_0$ can be obtained from prior knowledge or estimated during the jamming reaction period when no interference signal is present [28]. Note that to estimate $\boldsymbol{h}_0$, there is no need to separately estimate the transmitter-IRS channel $\boldsymbol{u}$ and the IRS-receiver channel $\boldsymbol{q}$. Many existing methods were proposed to directly estimate the cascaded channel, e.g. [13]–[17].

Note that the above model is a narrowband model which holds valid when $\delta_\tau B \ll 1$, where B denotes the receiver bandwidth and δ_τ denotes the delay spread of the channel between a source and the receiver. Given $\delta_\tau B \ll 1$, we can arrive at the above narrowband model even when the interference signal has a bandwidth far greater than B. A detailed derivation of this narrowband signal model is provided in Appendix A.

Our objective is to adaptively adjust the reflection vector $\boldsymbol{v}$ (i.e. $\boldsymbol{a}$) in order to nullify the received interference signals and guarantee the successful recovery of the desired signal $s(t)$. Such a problem finds a variety of applications in wireless communications, radar and other fields.

B. Problem Formulation

For noncooperative interference sources, it is challenging to estimate the cascaded interference channels. To address this difficulty, a natural strategy for interference cancelation is to find a reflection vector $\boldsymbol{v}$ to minimize the average received signal power, meanwhile subject to a received power constraint placed on the desired signal:

$$\begin{aligned} \min_{\boldsymbol{v}} \quad & \mathbb{E}[|y(t)|^2] \\ \text{s.t.} \quad & \boldsymbol{a}^H \boldsymbol{h}_0 = \gamma, \\ & \boldsymbol{a} = [1 \;\; \boldsymbol{v}^H]^H, \\ & |v_l| \le 1, \quad \forall l = 1, \ldots, L \end{aligned} \tag{4}$$

where $y(t)$ is defined in (1), the first constraint is equivalent to placing a received signal power constraint on the desired signal, γ is a pre-specified constant, v_l denotes the lth entry of $\boldsymbol{v}$, and $|v_l| = \beta_l \le 1$ is a constraint placed on the reflection coefficient such that the reflection amplitude β_l cannot exceed 1. Based on Assumptions A1–A2, the average received signal power $\mathbb{E}[|y(t)|^2]$ can be expressed as

$$\begin{aligned} \mathbb{E}[|y(t)|^2] =& \boldsymbol{a}^H \underbrace{\left(\boldsymbol{h}_0 \boldsymbol{h}_0^H\right)}_{\boldsymbol{R}_0} \boldsymbol{a} + \boldsymbol{a}^H \underbrace{\left(\sum_{k=1}^K \sigma_k^2 \boldsymbol{h}_k \boldsymbol{h}_k^H\right)}_{\boldsymbol{R}_J} \boldsymbol{a} + \sigma_w^2, \\ =& \boldsymbol{a}^H \boldsymbol{R}_0 \boldsymbol{a} + \boldsymbol{a}^H \boldsymbol{R}_J \boldsymbol{a} + \sigma_w^2, \\ =& \boldsymbol{a}^H \boldsymbol{R} \boldsymbol{a} + \sigma_w^2, \end{aligned} \tag{5}$$

where $\boldsymbol{R} \triangleq \boldsymbol{R}_0 + \boldsymbol{R}_J$ is the signal-plus-interference covariance matrix.

Hence, the problem (4) can be further simplified as

$$\begin{aligned} \min_{\boldsymbol{a}} \quad & \boldsymbol{a}^H \boldsymbol{R} \boldsymbol{a} \\ \text{s.t.} \quad & \boldsymbol{a}^H \boldsymbol{h}_0 = \gamma, \\ & |v_l| \le 1, \quad \forall l = 1, \ldots, L \end{aligned} \tag{6}$$

By ignoring the constraints $|v_l| \le 1$, we see that the above problem has a form similar to canonical ABF in array signal processing. Nevertheless, there is an important distinction between these two problems. For conventional ABF, the covariance matrix $\boldsymbol{R}$ is assumed known *a priori* since it can be readily estimated from the received signal samples. In contrast, for our considered problem, $\boldsymbol{R}$ is not directly available. Instead, the receiver can only observe quadratic compressive measurements of $\boldsymbol{R}$, i.e. $\{z_i \triangleq \boldsymbol{a}_i^H \boldsymbol{R} \boldsymbol{a}_i\}$, i.e., we can configure the IRS with a pre-designed augmented reflection vector $\boldsymbol{a}_i$ and then measure its average received signal power at the receiver, which yields a quadratic compressive measurement of $\boldsymbol{R}$: $z_i \triangleq \boldsymbol{a}_i^H \boldsymbol{R} \boldsymbol{a}_i$. Overall, the lack of the knowledge of $\boldsymbol{R}$ imposes a great challenge for solving (6).

A straightforward approach to address the above problem is to estimate $\boldsymbol{R}$ first and then solve (6) using the estimated $\boldsymbol{R}$. In fact, estimating a covariance matrix from its quadratic sketches $\{z_i\}$ is known as "covariance sketching" and has been investigated in some prior works, e.g. [24], [26]. It was reported in [26] that the number of measurements (i.e. quadratic sketches) should exceed the order of $\mathcal{O}((L+1)(K+1)^4)$ to recover the covariance matrix $\boldsymbol{R}$ with theoretical guarantees. Such a sample complexity, however, is excessive for practical applications. Note that $\boldsymbol{R}$, a function of the channel vectors $\{\boldsymbol{h}_k\}$, changes as the wireless channels vary. Therefore, the covariance matrix $\boldsymbol{R}$ should be estimated within a time duration that is smaller than the channel coherence time

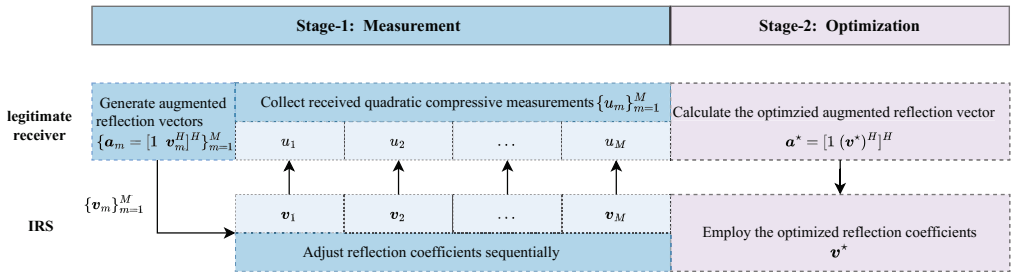

Fig. 2. General framework for the proposed method.

so that the estimated $\boldsymbol{R}$ will not become obsolete. Considering the fact that the channel coherence time is usually small, it is almost impossible to collect as many quadratic sketches of $\boldsymbol{R}$ as required for recovering $\boldsymbol{R}$.

To address the above difficulty, we will develop a sample-efficient solution to solve (6) without explicitly inferring $\boldsymbol{R}$.

III. Proposed ABF Method

To facilitate the exposition of our idea, we first ignore the amplitude constraint $|v_l| \leq 1, \forall l$ placed on the reflecting elements. We will discuss in the next section how to extend the proposed method to realize ABF with amplitude constraints. By neglecting the amplitude constraints, problem (6) can be simplified as

$$\begin{aligned} \min_{\boldsymbol{a}} \quad & \boldsymbol{a}^H \boldsymbol{R} \boldsymbol{a} \\ \text{s.t.} \quad & \boldsymbol{a}^H \boldsymbol{h}_0 = \gamma, \\ & \boldsymbol{a} = [1\ \ \boldsymbol{v}^H]^H. \end{aligned} \tag{7}$$

Clearly, the optimum solution $\boldsymbol{a}^\star$ to (7) should satisfy the following conditions:

$$(\boldsymbol{a}^\star)^H \boldsymbol{R}_J \boldsymbol{a}^\star = 0, \tag{8}$$

$$(\boldsymbol{a}^\star)^H \boldsymbol{h}_0 = \gamma. \tag{9}$$

It is evident that the optimal $\boldsymbol{a}^\star$ must lie in the null space of $\boldsymbol{R}_J$. While obtaining $\boldsymbol{a}^\star$ is straightforward if $\boldsymbol{R}_J$ is known, the challenge lies in that the knowledge of $\boldsymbol{R}_J$ is unavailable. Since estimating $\boldsymbol{R}_J = \boldsymbol{R} - \boldsymbol{R}_0$ is sample costly, we attempt to directly find a vector $\boldsymbol{a}$ that satisfies (8)–(9) without explicitly inferring $\boldsymbol{R}$ or $\boldsymbol{R}_J$.

Before proceeding to the detailed development of the algorithm, we first provide a general framework for the proposed method. Specifically, as illustrated in Fig. 2, the proposed method consists of a measurement stage and an optimization stage. The objective of the measurement stage is to collect a set of quadratic compressive measurements of $\boldsymbol{R}_J$. Specifically, in the measurement stage, the receiver first constructs a set of reflection vectors $\{\boldsymbol{v}_m\}_{m=1}^M$. Here, M denotes the number of quadratic compressive measurements collected during the measurement stage. These reflection vectors are then successively configured to the IRS. For each reflection vector $\boldsymbol{v}_m$, the receiver calculates its average received signal power:

$$\hat{z}_m = \frac{1}{T} \sum_{t=1}^{T} |y_m(t)|^2 \approx \boldsymbol{a}_m^H \boldsymbol{R}_0 \boldsymbol{a}_m + \boldsymbol{a}_m^H \boldsymbol{R}_J \boldsymbol{a}_m + \sigma_w^2, \tag{10}$$

where $\boldsymbol{a}_m \triangleq [1\ \ \boldsymbol{v}_m^H]^H$, $y_m(t)$ denotes the tth received data sample when the reflection vector $\boldsymbol{v}_m$ is employed, and T denotes the total number of data samples used to calculate the average received signal power. As $\boldsymbol{R}_0 = \boldsymbol{h}_0 \boldsymbol{h}_0^H$ is known and the noise variance σ_w^2 can be estimated *a priori*, from $\hat{z}_m$ we can obtain an estimate of $\boldsymbol{a}_m^H \boldsymbol{R}_J \boldsymbol{a}_m$:

$$u_m = \boldsymbol{a}_m^H \boldsymbol{R}_J \boldsymbol{a}_m + n_m, \tag{11}$$

where n_m is used to represent the estimation error.

Based on the collected quadratic compressive measurements $\{u_m\}_{m=1}^M$, the optimization stage calculates an augmented reflection vector that satisfies (8)–(9). In the following, we will delve into the details of the proposed method. Particularly, we will show how to construct these M reflection vectors $\{\boldsymbol{a}_m\}_{m=1}^M$ that are used in the measurement stage, and based on the measured data $\{u_m\}_{m=1}^M$, how to determine an optimal augmented reflection vector that satisfies (8)–(9).

A. Problem Simplification

The objective of this subsection is to reduce the dimensionality of problem (7) by leveraging the low-rank property of $\boldsymbol{R}_J$.

First, define $\boldsymbol{H} \triangleq [\boldsymbol{h}_1\ \ \boldsymbol{h}_2\ \ \ldots\ \ \boldsymbol{h}_K] \in \mathbb{C}^{(L+1)\times K}$. It can be easily verified that (8) is equivalent to

$$\boldsymbol{H}^H \boldsymbol{a}^\star = \boldsymbol{0}. \tag{12}$$

We first randomly generate I $(L+1 \gg I > K)$ mutually independent vectors $\{\tilde{\boldsymbol{a}}_i\}_{i=1}^I$ that are linearly independent of $\boldsymbol{h}_0$. Define

$$\boldsymbol{A} \triangleq [\boldsymbol{h}_0\ \ \tilde{\boldsymbol{a}}_1\ \ \tilde{\boldsymbol{a}}_2\ \ \ldots\ \ \tilde{\boldsymbol{a}}_I] \in \mathbb{C}^{(L+1)\times(I+1)}. \tag{13}$$

We will show that the vector $\boldsymbol{a}^\star$ which satisfies (8)–(9) can be obtained as a linear combination of columns of $\boldsymbol{A}$, i.e. $\boldsymbol{a}^\star = \boldsymbol{A}\boldsymbol{w}^\star$.

Define $\boldsymbol{T} \triangleq \boldsymbol{H}^H \boldsymbol{A} \in \mathbb{C}^{K\times(I+1)}$. Since $I > K$, there must exist a nonzero vector $\boldsymbol{w}^\star$ such that $\boldsymbol{T}\boldsymbol{w}^\star = \boldsymbol{0}$, which means that $\boldsymbol{H}^H \boldsymbol{A}\boldsymbol{w}^\star = \boldsymbol{0}$. Hence, $\boldsymbol{A}\boldsymbol{w}^\star$ satisfies (12), and consequently (8). Note that since $\{\tilde{\boldsymbol{a}}_i\}_{i=1}^I$ are mutually independent and $L+1 > I$, $\boldsymbol{A}$ is a matrix of full column rank.

Therefore $\boldsymbol{A}\boldsymbol{w}$ must be a nonzero vector for any $\boldsymbol{w} \neq \boldsymbol{0}$. On the other hand, if the matrix $\boldsymbol{A}$ has linearly dependent columns, the augmented reflection vector $\boldsymbol{a}^\star = \boldsymbol{A}\boldsymbol{w}^\star$ could be a zero vector even for a nonzero solution $\boldsymbol{w}^\star$, which is undesirable. This is the reason why we need to construct a full column-rank matrix $\boldsymbol{A}$.

Substituting $\boldsymbol{a}^\star = \boldsymbol{A}\boldsymbol{w}^\star$ into (9), we have

$$(\boldsymbol{w}^\star)^H \boldsymbol{A}^H \boldsymbol{h}_0 = \gamma. \tag{14}$$

So far we have shown that the vector $\boldsymbol{a}^\star$ which satisfies (8)–(9) can be expressed in a form of $\boldsymbol{a}^\star = \boldsymbol{A}\boldsymbol{w}^\star$. The problem now becomes, given a pre-specified $\boldsymbol{A}$, how to find a vector $\boldsymbol{w}^\star$. To this objective, substituting $\boldsymbol{a}^\star = \boldsymbol{A}\boldsymbol{w}^\star$ into (8), we arrive at

$$(\boldsymbol{w}^\star)^H \boldsymbol{A}^H \boldsymbol{R}_J \boldsymbol{A}\boldsymbol{w}^\star = (\boldsymbol{w}^\star)^H \boldsymbol{G}\boldsymbol{w}^\star = 0. \tag{15}$$

where $\boldsymbol{G} \triangleq \boldsymbol{A}^H \boldsymbol{R}_J \boldsymbol{A} \in \mathbb{C}^{(I+1)\times(I+1)}$ is a compressive observation of the covariance matrix $\boldsymbol{R}_J \in \mathbb{C}^{(L+1)\times(L+1)}$. From (15), we know that once $\boldsymbol{G}$ is known, $\boldsymbol{w}^\star$ can be accordingly determined. Therefore our objective in the following is to recover $\boldsymbol{G}$. Note that since $\boldsymbol{G}$ has a dimension much smaller than the dimension of $\boldsymbol{R}_J$, recovering $\boldsymbol{G}$ is more amiable than recovering $\boldsymbol{R}_J$ in terms of sample complexity.

B. Recover Matrix $\boldsymbol{G}$

Specifically, considering the Hermitian property of $\boldsymbol{G}$, we only need to recover the diagonal and half of its off-diagonal elements. To this goal, we generate a set of augmented reflection vectors according to

$$\boldsymbol{a}_m = \boldsymbol{A}\boldsymbol{w}_m, \quad \forall m = 1, \ldots, M \tag{16}$$

where $\boldsymbol{w}_m = [w_{m,1} \;\; w_{m,2} \;\; \ldots \;\; w_{m,(I+1)}]^T$. These M vectors $\{\boldsymbol{w}_m\}_{m=1}^M$ can be randomly generated as long as the first element of each $\boldsymbol{a}_m$ is equal to 1, as required by its definition. As discussed earlier, these M augmented reflection vectors $\{\boldsymbol{a}_m\}_{m=1}^M$ are then used in the measurement stage to obtain a set of measurements $\{u_m\}_{m=1}^M$.

Combining (16) and (11), we have

$$\begin{aligned}
u_m =& \boldsymbol{w}_m^H \boldsymbol{G}\boldsymbol{w}_m + n_m, \\
=& \sum_{i=1}^{I+1}\sum_{j=1}^{I+1} w_{m,i}^* G_{i,j} w_{m,j} + n_m, \\
=& \sum_{i=1}^{I+1} |w_{m,i}|^2 G_{i,i} + 2\sum_{i=1}^{I+1}\sum_{j>i}^{I+1} \Re\{w_{m,i}^* w_{m,j} G_{i,j}\} + n_m, \\
=& \sum_{i=1}^{I+1} |w_{m,i}|^2 G_{i,i} + 2\sum_{i=1}^{I+1}\sum_{j>i}^{I+1} \Big(\Re\{w_{m,i}^* w_{m,j}\}\Re\{G_{i,j}\} \\
& - \Im\{w_{m,i}^* w_{m,j}\}\Im\{G_{i,j}\} \Big) + n_m,
\end{aligned} \tag{17}$$

where G_{ij} denotes the (i,j)th element of $\boldsymbol{G}$, $\Re\{\cdot\}$ and $\Im\{\cdot\}$ respectively denote the real and imaginary components of a complex number.

To re-express (17) into a more tractable form, we re-arrange the elements in $\boldsymbol{G}$ and $\boldsymbol{w}_m$. Let

$$\boldsymbol{g}_d = [G_{1,1} \;\; G_{2,2} \;\; \ldots \;\; G_{I+1,I+1}]^T \tag{18}$$

denote a vector consisting of the diagonal elements of $\boldsymbol{G}$. Let

$$\boldsymbol{g}_{d,i} \triangleq [G_{1,1+i} \;\; G_{2,2+i} \;\; \ldots \;\; G_{I+1-i,I+1}]^T \in \mathbb{C}^{I+1-i}, \quad i = 1, 2, \ldots, I \tag{19}$$

denote a vector comprised of the ith superdiagonal entries of $\boldsymbol{G}$. Put all elements above the main diagonal of $\boldsymbol{G}$ into a vector as

$$\boldsymbol{g}_{o-d} = [\boldsymbol{g}_{d,1}^T \;\; \boldsymbol{g}_{d,2}^T \;\; \ldots \;\; \boldsymbol{g}_{d,I}^T]^T \in \mathbb{C}^{\frac{I(I+1)}{2}}. \tag{20}$$

Finally, the matrix $\boldsymbol{G}$ can be characterized by a vector defined as

$$\boldsymbol{g} = [\boldsymbol{g}_d^T \;\; \Re\{\boldsymbol{g}_{o-d}\}^T \;\; \Im\{\boldsymbol{g}_{o-d}\}^T]^T \in \mathbb{R}^{(I+1)^2}, \tag{21}$$

Clearly, the vector $\boldsymbol{g}$ consists of $(I+1) + 2\times(I(I+1)/2) = (I+1)^2$ entries.

Define $\bar{\boldsymbol{W}}_m \triangleq \boldsymbol{w}_m \boldsymbol{w}_m^H \in \mathbb{C}^{(I+1)\times(I+1)}$. Similarly, we define a vector $\bar{\boldsymbol{w}}_m \in \mathbb{C}^{(I+1)^2}$ as

$$\bar{\boldsymbol{w}}_m = [\bar{\boldsymbol{w}}_{m,d}^T \;\; 2\Re\{\bar{\boldsymbol{w}}_{m,o-d}\}^T \;\; 2\Im\{\bar{\boldsymbol{w}}_{m,o-d}\}^T]^T. \tag{22}$$

where $\bar{\boldsymbol{w}}_{m,d} \in \mathbb{R}^{(I+1)}$ is a vector consisting of the main diagonal elements of $\bar{\boldsymbol{W}}_m$, and $\bar{\boldsymbol{w}}_{m,o-d} \in \mathbb{C}^{I(I+1)/2}$ is a vector consisting of entries above the main diagonal of $\bar{\boldsymbol{W}}_m$.

Based on the above notations, (17) can be written in a compact form as

$$u_m = \bar{\boldsymbol{w}}_m^T \boldsymbol{g} + n_m \tag{23}$$

Note that for each $\boldsymbol{a}_m = \boldsymbol{A}\boldsymbol{w}_m$, we can obtain its corresponding measurement u_m and construct the corresponding vector $\bar{\boldsymbol{w}}_m$ from $\boldsymbol{w}_m$. The collected measurements $\{u_m\}_{m=1}^M$ are then used in the optimization stage to find an optimal augmented reflection vector $\boldsymbol{a}^\star$. By stacking the measurements $\{u_m\}_{m=1}^M$, we have

$$\boldsymbol{u} \triangleq \begin{bmatrix} u_1 \\ u_2 \\ \vdots \\ u_M \end{bmatrix} = \begin{bmatrix} \bar{\boldsymbol{w}}_1^T \\ \bar{\boldsymbol{w}}_2^T \\ \vdots \\ \bar{\boldsymbol{w}}_M^T \end{bmatrix} \boldsymbol{g} + \begin{bmatrix} n_1 \\ n_2 \\ \vdots \\ n_M \end{bmatrix} = \boldsymbol{W}\boldsymbol{g} + \boldsymbol{n}. \tag{24}$$

There exists $(I+1)^2$ unknown variables in the above equation. By choosing $M \geq (I+1)^2$ and letting $\{\boldsymbol{w}_m\}_{m=1}^M$ linearly independent, the unknown vector $\boldsymbol{g}$ can be estimated via a simple least-squares (LS) method, i.e.,

$$\hat{\boldsymbol{g}} = \boldsymbol{W}^\dagger \boldsymbol{u}, \tag{25}$$

where $\boldsymbol{W}^\dagger$ denotes the Moore-Penrose inverse of $\boldsymbol{W}$. After $\boldsymbol{g}$ is estimated, the matrix $\boldsymbol{G}$ can be accordingly recovered.

C. Determining $\boldsymbol{w}^\star$

After recovering $\boldsymbol{G}$, we now discuss how to obtain $\boldsymbol{w}^\star$. Note that $\boldsymbol{w}^\star$ needs to satisfy (15). Also, the vector $\boldsymbol{w}^\star$ is supposed to meet (14) in order to satisfy (9). In addition, notice that we have to make sure that the first entry of $\boldsymbol{a}^\star = \boldsymbol{A}\boldsymbol{w}^\star$ is equal to one, as required by the definition of the augmented reflection vector $\boldsymbol{a}$.

In the following, we discuss how to obtain $\boldsymbol{w}^\star$ to meet the above requirements. Since different channels are linearly independent, the rank of $\boldsymbol{G} = \boldsymbol{A}^H \boldsymbol{R}_J \boldsymbol{A}$ is equal to K. Thus,

the null space of $\boldsymbol{G} \in \mathbb{C}^{(I+1)\times(I+1)}$ has a dimension of $I+1-K \geq 2$. For simplicity, denote $\boldsymbol{z}_1$ and $\boldsymbol{z}_2$ as two basis vectors of the null space of $\boldsymbol{G}$. Thus, we can express

$$\boldsymbol{w}^\star = \varrho_1 \boldsymbol{z}_1 + \varrho_2 \boldsymbol{z}_2 \tag{26}$$

Clearly, such a $\boldsymbol{w}^\star$ automatically satisfies (15). Here ϱ_1 and ϱ_2 are variables to be determined, such that the vector $\boldsymbol{w}^\star$ satisfies (14) and the first entry of $\boldsymbol{a}^\star = \boldsymbol{A}\boldsymbol{w}^\star$ equals to one, i.e.

$$\varrho_1 \boldsymbol{z}_1^H \boldsymbol{A}^H \boldsymbol{h}_0 + \varrho_2 \boldsymbol{z}_2^H \boldsymbol{A}^H \boldsymbol{h}_0 = \gamma, \tag{27}$$

$$\varrho_1 [\boldsymbol{A}\boldsymbol{z}_1]_1 + \varrho_2 [\boldsymbol{A}\boldsymbol{z}_2]_1 = 1, \tag{28}$$

where $[\boldsymbol{A}\boldsymbol{z}_1]_1$ and $[\boldsymbol{A}\boldsymbol{z}_2]_1$ represent the first elements of the vectors $\boldsymbol{A}\boldsymbol{z}_1$ and $\boldsymbol{A}\boldsymbol{z}_2$, respectively. From the above equations, the variables ϱ_1 and ϱ_2 can be readily determined.

Note that due to the presence of the estimation error $\boldsymbol{n}$, the estimated matrix $\hat{\boldsymbol{G}}$ may have a rank greater than K. This could cause a problem in obtaining the correct bases of the null space of $\hat{\boldsymbol{G}}$. To address this issue, we can increase the dimension of the matrix $\boldsymbol{G}$ by generating more mutually independent vectors $\{\tilde{\boldsymbol{a}}_i\}_{i=1}^I$. We can then choose the eigenvectors corresponding to the smallest eigenvalues as the basis vectors. In doing this way, the proposed method can enhance its numerical stability and robustness against estimation errors.

D. Summary

So far we have provided an analytical solution to problem (7). In summary, the proposed method first randomly generates $I > K$ independent vectors $\{\tilde{\boldsymbol{a}}_i\}$ and construct a matrix $\boldsymbol{A}$ according to (13). Then, it generates $M \geq (I+1)^2$ independent vectors $\{\boldsymbol{w}_m\}_{m=1}^M$. Based on $\{\boldsymbol{w}_m\}_{m=1}^M$, it calculates M reflection vectors $\{\boldsymbol{a}_m\}_{m=1}^M$ according to (16). These M reflection vectors are successively employed by the IRS. For each augmented reflection vector $\boldsymbol{a}_m$, the receiver calculates its average received signal power and obtains an estimate of u_m. After all measurements $\{u_m\}_{m=1}^M$ are obtained, we can recover the matrix $\boldsymbol{G}$ according to (25). Finally the weighting vector $\boldsymbol{w}^\star$ can be accordingly determined and the augmented reflection vector which satisfies (8)–(9) can be obtained as $\boldsymbol{a}^\star = \boldsymbol{A}\boldsymbol{w}^\star$. For clarity, we summarize the proposed method in Algorithm 1.

Note that the minimum value of I can be chosen as $I = K+1$. Therefore the proposed method requires a minimum of $M = (I+1)^2 = (K+2)^2$ measurements (i.e. quadratic sketches of $\boldsymbol{R}$) to find a qualified augmented reflection vector $\boldsymbol{a}^\star$. This sample complexity is independent of the number of reflecting elements of the IRS, and thus achieves a remarkable sample complexity reduction as compared to the covariance sketching method which aims to recover the covariance matrix $\boldsymbol{R}$. Specifically, if there is only a single interference signal, i.e. $K = 1$, then our proposed method only needs 9 measurements to identify an augmented reflection vector which nullifies the interference signal. Such a sample efficiency enables the proposed algorithm to accommodate fast-changing channel environments.

Remark: Note that the proposed method does not require the precise number of interference signals. Instead, an upper bound on the number of interference signals, i.e., $\bar{K}$, is enough for the proposed method. Specifically, we can choose $I > \bar{K}$ for our proposed method. This, however, leads to an increase in sample complexity from $(K+2)^2$ to $(\bar{K}+2)^2$ for the proposed method.

Algorithm 1 Proposed Solution for ABF

Inputs: K and M, first generate the measurement matrix $\boldsymbol{A}$ according to (13).

Do

Stage-1 (Measurement):

1. Randomly generate M linear independent vectors $\{\boldsymbol{w}_m\}_{m=1}^M$ and obtain the corresponding augmented reflection vectors $\{\boldsymbol{a}_m\}_{m=1}^M$ via $\boldsymbol{a}_m = \boldsymbol{A}\boldsymbol{w}_m$;

2. Estimate the average received signal power measurements $\{\hat{z}_m\}_{m=1}^M$ via (10) and then obtain $\{u_m\}_{m=1}^M$ based on the prior knowledge of $\boldsymbol{R}_0$ and σ_w^2;

Stage-2 (Optimization):

1. Obtain the vector $\hat{\boldsymbol{g}}$ via (25) and reshape it to recover $\boldsymbol{G}$;

3. Obtain the vector $\boldsymbol{w}^\star$ via solving (27) and (28) and obtain $\boldsymbol{a}^\star = \boldsymbol{A}\boldsymbol{w}^\star$ accordingly;

End

Output $\boldsymbol{a}^\star$;

IV. Realizing ABF via Passive IRS

In the previous section, to facilitate the exposition of our idea, we ignored the practical constraint imposed on the reflection coefficients. In practice, due to the passive nature of the IRS, the reflection amplitude β_l cannot exceed one. This means in Algorithm 1, the generated measurement vector $\{\boldsymbol{a}_m\}$ and the obtained optimal solution $\boldsymbol{a}^\star$ are supposed to satisfy the following constraints

$$a_{m,1} = 1,\ |a_{m,i}| \leq 1, \forall m = 1,2,\ldots,M, i = 2,3,\ldots,L+1, \tag{29}$$

$$a_1^\star = 1,\ |a_i^\star| \leq 1, \forall i = 2,3,\ldots,L+1, \tag{30}$$

where $a_{m,i}$ ($a_i^\star$) denote the ith element of $\boldsymbol{a}_m$ ($\boldsymbol{a}^\star$). The constraints $a_{m,1} = 1, \forall m$ and $a_1^\star = 1$ are a result of the definition $\boldsymbol{a} = [1\ \boldsymbol{v}^H]^H$, which has been considered in the design of Algorithm 1. Unfortunately, the reflection amplitude constraints $|a_{m,i}| \leq 1, \forall i = 2,\ldots,L+1$ and $|a_i^\star| \leq 1, \forall i = 2,\ldots,L+1$ were not considered by Algorithm 1. In the following, we will elaborate how to adapt our proposed solution to the passive IRS scenario.

A. Generating $\{\boldsymbol{a}_m\}_{m=1}^M$

In Algorithm 1, the first step is to generate M augmented reflection vectors $\{\boldsymbol{a}_m\}$, where $\boldsymbol{a}_m = \boldsymbol{A}\boldsymbol{w}_m, \forall m$. In the following, we propose an efficient method for generating a set of vectors $\{\boldsymbol{a}_m\}_{m=1}^M$ that satisfy the constraints specified in (29).

First of all, any vector $\boldsymbol{w}_m$ that satisfies the constraint $a_{m,1} = 1$ can be expressed as:

$$\boldsymbol{w}_m = \boldsymbol{w}_0 + \boldsymbol{D}\boldsymbol{d}_m, \tag{31}$$

where $\boldsymbol{w}_0$ is any vector satisfying $\boldsymbol{A}(1,:)\boldsymbol{w}_0 = 1$, $\boldsymbol{D} \in \mathbb{C}^{(I+1)\times I}$ is a matrix spanning the null space of $\boldsymbol{A}(1,:)$, i.e., $\boldsymbol{A}(1,:)\boldsymbol{D} = \boldsymbol{0}$, and $\boldsymbol{d}_m \in \mathbb{C}^I$ is an arbitrary vector.

Our goal is to generate a set of vectors $\{\boldsymbol{d}_m\}_{m=1}^M$ such that the amplitude of each entry in the vector $\boldsymbol{a}_m = \boldsymbol{A}\boldsymbol{w}_m = \boldsymbol{A}\boldsymbol{w}_0 + \boldsymbol{A}\boldsymbol{D}\boldsymbol{d}_m$ remains within the unit circle, i.e., less than 1. To this goal, we first normalize the matrix $\boldsymbol{A}$ such that $\|\boldsymbol{A}\|_F = 1$. Subsequently, we generate each vector $\boldsymbol{d}_m$ by drawing samples from a complex Gaussian distribution with zero mean and unit variance.

After generating $\boldsymbol{d}_m$, we check whether the constraint $|a_{m,i}| \leq 1$ is satisfied for all $i = 2, 3, \ldots, L+1$. If the constraint is not met, we normalize the vector $\boldsymbol{d}_m$ as follows:

$$\tilde{\boldsymbol{d}}_m = \boldsymbol{d}_m \frac{d_{\min}}{d_{\max}}, \tag{32}$$

where

$$b_i \triangleq \boldsymbol{A}(i,:)\boldsymbol{w}_0, \quad d_{\min} = \min_{i=2,\ldots,L+1} \quad 1 - |b_i|, \tag{33}$$

$$d_{\max} = \max_{i=2,\ldots,L+1} \quad |\boldsymbol{A}(i,:)\boldsymbol{D}\boldsymbol{d}_m|. \tag{34}$$

By setting $\|\boldsymbol{A}\|_F = 1$, we can ensure $d_{\min} \geq 0$ with a high probability.

Henceforth, the magnitude of the ith ($L+1 \geq i \geq 2$) entry of the measurement vector $\boldsymbol{a}_m$ can be upper bounded by

$$\begin{aligned} |a_{m,i}| =& |b_i + \boldsymbol{A}(i,:)\boldsymbol{D}\tilde{\boldsymbol{d}}_m| \\ =& |b_i + \frac{d_{\min}}{d_{\max}}\boldsymbol{A}(i,:)\boldsymbol{D}\boldsymbol{d}_m|, \\ \overset{(a)}{\leq}& |b_i| + \left|\frac{d_{\min}}{d_{\max}}\right| |\boldsymbol{A}(i,:)\boldsymbol{D}\boldsymbol{d}_m|, \\ \leq& |b_i| + |d_{\min}| \leq 1, \end{aligned} \tag{35}$$

where (a) comes from the triangle inequality.

B. Identifying $\boldsymbol{a}^\star$

In addition to the measurement vectors $\{\boldsymbol{a}_m\}$, we also need to ensure that the vector $\boldsymbol{a}^\star$ satisfies the constraints (30). In other words, we need to determine a vector $\boldsymbol{w}^\star$ such that the resulting vector $\boldsymbol{a}^\star = \boldsymbol{A}\boldsymbol{w}^\star$ not only satisfies (8)–(9), but also (30). To this objective, we need to make sure that the dimension of the null space of $\boldsymbol{G}$, denoted as $P = I+1-K$, is greater than 3, i.e. $P = I+1-K \geq 3$.

Let $\boldsymbol{Z} \in \mathbb{C}^{(I+1)\times P}$ be a matrix comprising P basis vectors of the null space of $\boldsymbol{G}$. Then, $\boldsymbol{w}^\star$ can be expressed as:

$$\boldsymbol{w}^\star = \boldsymbol{Z}\boldsymbol{t}^\star. \tag{36}$$

Denote $\boldsymbol{B} \triangleq \boldsymbol{A}\boldsymbol{Z}$. Then, the problem of finding $\boldsymbol{a}^\star = \boldsymbol{A}\boldsymbol{w}^\star = \boldsymbol{B}\boldsymbol{t}^\star$ is equivalent to:

$$\begin{aligned} \text{find} \quad & \boldsymbol{t} \\ \text{s.t.} \quad & \boldsymbol{B}(1,:)\boldsymbol{t} = 1, \\ & \boldsymbol{h}_0^H\boldsymbol{B}\boldsymbol{t} = \gamma, \\ & \|\boldsymbol{B}\boldsymbol{t}\|_\infty \leq 1. \end{aligned} \tag{37}$$

This problem is convex and can be efficiently solved using CVX tools [29]. For clarity, the proposed solution for passive IRS scenarios is summarized in Algorithm 2.

It should be noted that the problem in (37) may not always be feasible. There are several factors which have an effect on the feasibility of (37). First, due to the product path loss effect introduced by the IRS, the power of the reflected link could be much lower than that of the direct link. In this case, it is crucial to equip the IRS with a sufficient number of reflecting elements to form an adequate beamforming gain such that the direct link and the reflected link can cancel each other out. Of course, this issue can be alleviated if the direct link between the interference source and the receiver suffers a similar path loss due to the lack of the line-of-sight (LOS) component. Second, the problem in (37) may be infeasible for a small value of P, as the limited degrees of freedom restrict the ability to devise a vector $\boldsymbol{t}$ that satisfies all constraints. Increasing P can significantly enhance the feasibility of (37). Finally, the parameter γ must be carefully selected to ensure that the desired gain does not exceed the system's capability.

Algorithm 2 Proposed Solution for ABF using a passive IRS

Inputs: K and M. Generate the measurement matrix $\boldsymbol{A}$ according to (13) and normalize $\boldsymbol{A}$ to a unit Frobenius norm;

Do

Stage-1 (Measurement):

1. Obtain an arbitrary solution $\boldsymbol{w}_0$ to $\boldsymbol{A}(1,:)\boldsymbol{w}_0 = 1$;

2. Randomly generate M linear independent vectors $\{\boldsymbol{d}_m\}_{m=1}^M$ and obtain $\{\boldsymbol{a}_m\}_{m=1}^M$ via $\boldsymbol{a}_m = \boldsymbol{A}\boldsymbol{w}_0 + \boldsymbol{A}\boldsymbol{D}\tilde{\boldsymbol{d}}_m$;

3. Estimate the average received signal power measurements $\{\hat{z}_m\}_{m=1}^M$ via (10) and then obtain $\{u_m\}_{m=1}^M$ based on the prior knowledge of $\boldsymbol{R}_0$ and σ_w^2;

Stage-2 (Optimization):

1. Obtain the vector $\hat{\boldsymbol{g}}$ via (25) and reshape it to recover $\boldsymbol{G}$;

2. Obtain the vector $\boldsymbol{w}^\star$ or $\boldsymbol{t}^\star$ via solving (37) and calculate $\boldsymbol{a}^\star$ as $\boldsymbol{a}^\star = \boldsymbol{A}\boldsymbol{w}^\star = \boldsymbol{B}\boldsymbol{t}^\star$;

End

Output $\boldsymbol{a}^\star$;

C. Summary

So far, we have discussed how to extend our proposed method to solve the ABF problem for the passive IRS scenario. As discussed in Section III-D, we need a minimum number of measurements $M \geq (I+1)^2$ to recover $\boldsymbol{G}$. For the passive IRS scenario, to provide a sufficient degrees of freedom in solving (37), I is set to $I = P+K-1$. Therefore, for the passive IRS scenario, the minimum number of measurements required by our proposed method is $M \geq (P+K)^2$.

For our proposed method, the dominant computational complexity comes from solving (24) and (37). For (24), obtaining a LS solution involves a computational complexity at the order of $\mathcal{O}((I+1)^3)$. For problem (37), it can be transformed into $2 + 2P = 2 + 2(I+1-K) = 2(I-K)$ linear constraints. Thus, it has a computational complexity at the order of

$\mathcal{O}(8(I-K)^3\log(1/\epsilon))$, where ϵ is the desired precision. As a result, the overall computational complexity of the proposed solution is at the order of $\mathcal{O}((I+1)^3+8(I-K)^3\log(1/\epsilon))$.

V. Simulation Results

We now provide simulation results to illustrate the performance of the proposed IRS-assisted ABF method. In our simulations, the direct-link channel from the legitimate transmitter to the receiver r and the direct-link channel from each interference source to the receiver $g_k, \forall k$ are assumed to be Rayleigh fading channels and generated according to

$$h = \sqrt{\rho_0 D^{-\alpha}}u, \tag{38}$$

where $\rho_0 = -30$ dB, D denotes the distance between the transmitter and the receiver, α represents the path loss exponent, and $u \sim \mathcal{CN}(0,1)$. In our simulations, the path loss exponents for both the legitimate transmitter-receiver link and the interference sources-receiver link are set to 4.5 [30]. The IRS-associated channels, including those from the legitimate transmitter or the interference sources to the IRS and the channel from the IRS to the receiver, are generated by following the Saleh-Valenzuela model

$$\begin{aligned}\boldsymbol{h} =&\sqrt{\rho_0 D^{-\alpha}}\bigg(\sqrt{\frac{K_f}{K_f+1}}\beta_0\boldsymbol{b}_I(\theta_{a,0},\theta_{e,0})\\ &+\sqrt{\frac{1}{K_f+1}}\sum_{q=1}^{Q-1}\beta_q\boldsymbol{b}_I(\theta_{a,q},\theta_{e,q})\bigg),\end{aligned} \tag{39}$$

where K_f is the K-factor representing the ratio of the power of the LOS path to that of the non-line-of-sight (NLOS) paths, $\theta_{a,q}$ ($\theta_{e,q}$) denote the azimuth (elevation) angles of arrival/departure (AoA/AoD), and

$$\begin{aligned}\boldsymbol{b}_I(\theta_a,\theta_e) =&[1,\ldots,e^{j\pi(m-1)\sin(\theta_a)},\ldots,e^{j\pi(L_x-1)\sin(\theta_a)}]^T\\ &\otimes[1,\ldots,e^{j\pi(n-1)\cos(\theta_e)},\ldots,e^{j\pi(L_y-1)\cos(\theta_e)}]^T\end{aligned} \tag{40}$$

is the steering vector at the IRS, with L_x and L_y being the number of reflecting elements along the x- and y-dimension of the IRS, and Q denotes the number of paths. In our experiments, the path loss exponents for the legitimate transmitter-IRS link and the IRS-receiver link are set to 2, with a K-factor of 10 dB. The number of paths for the legitimate transmitter-IRS link and the IRS-receiver link is set to 2 and 3, respectively.

Without loss of generality, the transmit power of the legitimate transmitter is set to 0 dB, or equivalently 30 dBm, i.e., $\mathbb{E}[|s(t)|^2]=1$. The number of interference signals is set to $K=1$ unless otherwise specified. The number of the IRS's reflecting elements is set to $L = L_x \times L_y = 5\times 8 = 40$, and the noise power is set to -107 dBm across all experiments. To better illustrate the efficiency of the proposed algorithm, we include the following three methods for comparison.

The first one is the maximum ratio transmission (MRT) solution which simply sets the augmented reflection vector as $\boldsymbol{a}^\star_{\rm MRT} = \tilde{\boldsymbol{h}}_0/\tilde{\boldsymbol{h}}_0(1)$, with $\tilde{\boldsymbol{h}}_0 \triangleq \exp(j\arg(\boldsymbol{h}_0))$, $\arg(\cdot)$ being the argument of a complex number and $\tilde{\boldsymbol{h}}_0(1)$ denoting the first element of $\tilde{\boldsymbol{h}}_0$. We see that the MRT solution completely ignores the interference signals, and simply utilizes the knowledge of the channel $\boldsymbol{h}_0$ to maximize the receive power of the desired signal.

Another two competing methods solve the ABF problem via directly recovering the covariance matrix $\boldsymbol{R}$ from its quadratic compressive measurements $\{\hat{z}_m\}$. The first one estimates $\boldsymbol{R}$ via a LS method. It can be readily verified that the LS method requires at least $M > (L+1)^2 = 1681$ measurements to recover the covariance matrix $\boldsymbol{R}$. The second one recovers $\boldsymbol{R}$ via a covariance sketching (CS) method [26] which utilizes the low-rank structure of $\boldsymbol{R}$. Specifically, the work [26] develops a gradient descent method to find a low-rank $\boldsymbol{R}$ by minimizing the data fitting error. It should be noted that the CS method requires the prior knowledge the Frobenius norm of $\boldsymbol{R}$ to ensure convergence, a requirement that is not needed by other methods. After $\boldsymbol{R}$ is estimated, the augmented reflection vector can be obtained via solving (7) or (6). Note that for problem (6) where the amplitude constraints are considered, we need to follow a similar approach discussed in IV-B to find a qualified augmented reflection vector that satisfies the reflection amplitude constraints.

We evaluate the performance of respective algorithms via the signal-to-interference-plus-noise ratio (SINR) attained by each algorithm's augmented reflection vector $\boldsymbol{a}^\star$:

$$\text{SINR} \triangleq \frac{(\boldsymbol{a}^\star)^H\boldsymbol{R}_0\boldsymbol{a}^\star}{(\boldsymbol{a}^\star)^H\boldsymbol{R}_J\boldsymbol{a}^\star+\sigma_w^2} \tag{41}$$

In our experiments, γ is set to $0.6(\boldsymbol{a}^\star_{\rm MRT})^H\boldsymbol{h}_0$. Note that the value of γ should not be set too large, otherwise the problem (37) becomes infeasible. A reasonable range for γ can be determined based on the channel gain obtained by the MRT solution, i.e. $(\boldsymbol{a}^\star_{\rm MRT})^H\boldsymbol{h}_0$. Clearly, γ should not exceed the value of $(\boldsymbol{a}^\star_{\rm MRT})^H\boldsymbol{h}_0$. Specifically, we can choose $\gamma = \mu(\boldsymbol{a}^\star_{\rm MRT})^H\boldsymbol{h}_0$, where $0<\mu<1$. Our empirical results suggest that a conservative but reasonable choice of μ could be within the range of $[0.2, 0.6]$.

A. Scenarios Without Amplitude Constraints

We first verify the efficacy of the proposed Algorithm 1, which ignores the amplitude constraints placed on the reflection elements. In our experiments, the transmit power of each interference signal is set to 15 dB. The LS-based method and the CS method respectively use $M=1691$ and $M=820$ quadratic compressive measurements to solve the ABF problem. The total number of quadratic compressive measurements M used by our proposed method is set to $M=220$, and we choose $I = K+6 = 7$ to obtain a sufficiently large dimension for the null space of the matrix $\boldsymbol{G}$, which helps enhance the robustness against estimation errors and noise.

Fig. 3(a) depicts the SINRs of respective algorithms versus the number of samples T. Here T is the number of samples used to estimate the average received signal power $\hat{z}_m$ (cf. (10)). Clearly, the more data samples are used, the more accurate estimate of the statistics $\hat{z}_m$ can be obtained, which in turn helps improve the interference suppression performance. We see that the proposed method and the LS method outperform the MRT solution by a big margin, and the performance

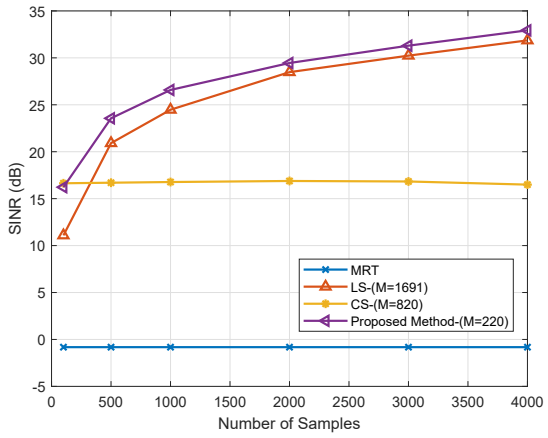

(a) SINR vs. the number of samples

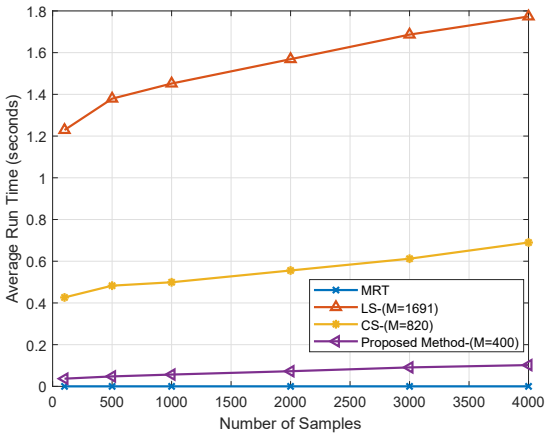

(b) Average run time vs. the number of samples

Fig. 3. SINR and Average run time vs. the number of samples

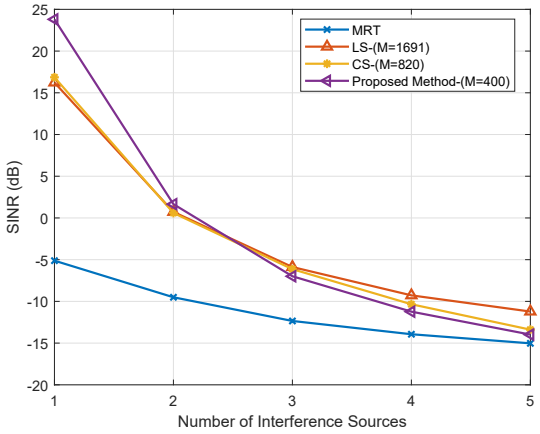

Fig. 4. SINR vs. Number of interference sources T.

gap becomes more pronounced as the number of sample increases. Also, the proposed method, even using much fewer measurements, achieves a performance advantage over the LS and CS methods. This result demonstrates the efficiency of the proposed method in suppressing the interference. We observe that the CS method does not perform as well as the other two methods, which may be attributed to the following reason. The CS method requires that the measurement vectors $\boldsymbol{a}_m$ are randomly generated according to a complex Gaussian distribution with zero mean and unit variance, a condition that cannot be met in our experiments since the first element of $\boldsymbol{a}_m$ is confined to be equal to 1. Fig. 3(b) plots the average run time of respective methods as a function of T. Note that we select the number of measurements, M, based on the conditions required for these methods to function properly. We see that the proposed method is much more computationally efficient than the LS and CS methods. For instance, when $T = 3000$, the proposed method requires only 0.09 seconds, compared to 0.61 and 1.67 seconds for the other two methods, respectively.

In Fig. 4, we plot the SINRs achieved by respective methods as a function of the number of interference signals K, where the transmit power of each interference source is set to 20 dB and the number of samples is set to $T = 500$. The number of measurements is set to $M = 400$ for our proposed method, and set to $M = 1691$ and $M = 820$ for the LS-based method and the CS method, respectively. As expected, all methods experience performance degradation as the number of interference signals increases. This is because the estimation of the averaged received signal power $\hat{z}_m$ becomes less accurate as the number of signals increases, which in turn affects the subsequent interference suppression performance.

B. Passive IRS Scenarios With Amplitude Constraints

We now present results to illustrate the performance of ABF achieved by using a passive IRS. For the passive IRS, the reflection amplitude of each reflecting element cannot exceed 1. In our experiments, we conduct 500 independent trials. In each trial, the direct link channels and IRS-associated channels are randomly generated according to (38) and (39), respectively. Occasionally for some trials we may not have a feasible solution to the problem (37). These unfeasible trials are excluded and we only average results over the successful trials in which the problem is feasible.

To better illustrate the effectiveness of the proposed algorithm, we also include the "random-max" method as a benchmark. For the random-max method, we first randomly generate a set of reflection coefficients, then we choose the one which achieves the highest SINR. Fig. 5 illustrates the performance of respective methods versus the interference source's transmit power, where we set the number of samples $T = 500$. The number of measurements for the CS method and the LS method are set to $M = 820$ and $M = 1691$, respectively. The number of measurements for our proposed method is set to $M = 220$ for $K = 1$ and $M = 235$

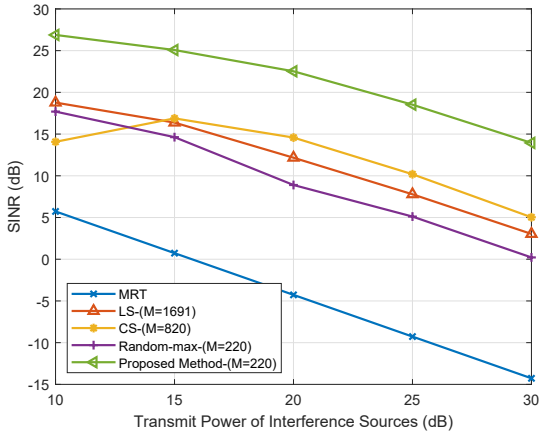

(a) SINR vs. the transmit power of interference source when $K = 1$.

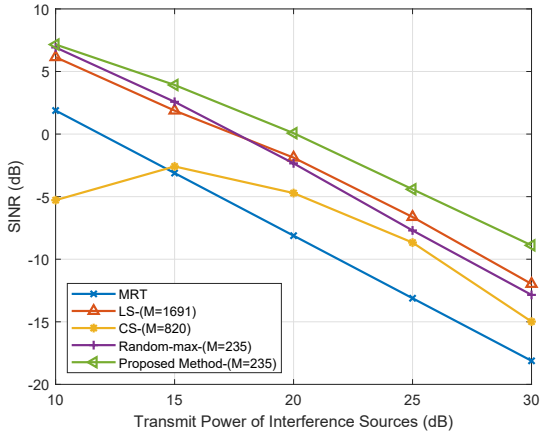

(b) SINR vs. the transmit power of interference source when $K = 2$.

Fig. 5. SINR vs. the transmit power of interference source for different number of interference sources.

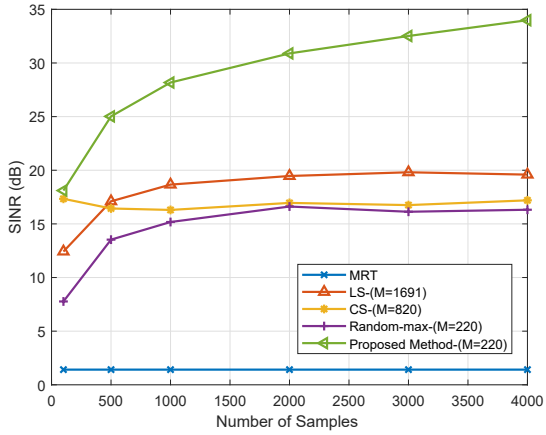

(a) SINR vs. the number of samples when $K = 1$.

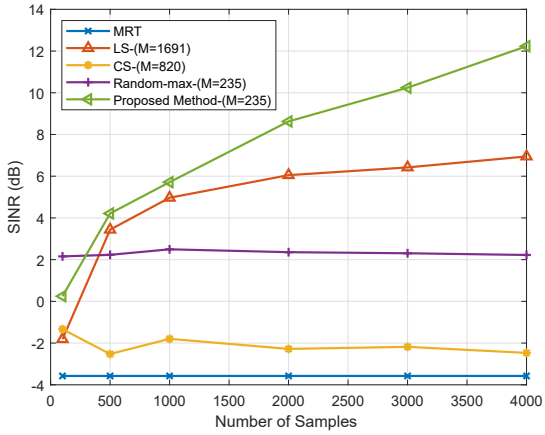

(b) SINR vs. the number of samples when $K = 2$.

Fig. 6. SINR vs. the number of samples for different number of interference sources.

for $K = 2$, where we set $I = K + 6$ for both cases. As shown in Fig. 5, when $K = 1$, the proposed method achieves an SINR improvement of nearly 21 dB as compared to the MRT solution. Moreover, the proposed method presents a clear improvement over the three competing algorithms across all transmit power levels.

Fig. 6 illustrates the SINRs achieved by respective methods as a function of the number of samples T. The transmit power of each interference source is set to 15 dB. We see that our proposed algorithm achieves a significant performance improvement as the number of samples T grows, whereas the gain obtained by the other competing algorithms with increasing T is marginal. For the case of $K = 2$, the CS method exhibits a severe performance degradation and achieves even a lower SINR than the random-max method, while the proposed method consistently outperforms the other approaches when $T \geq 500$.

C. Passive IRS: Beam Patterns

To illustrate how the proposed method improves SINR performance, we analyze beam patterns under different values of γ. The IRS is configured as a uniform linear array with $L = 8$ reflecting elements. For simplicity, the direct links between the legitimate/interfering transmitter and the receiver are assumed to be blocked, while the reflected links are dominated by line-of-sight (LoS) paths.

Fig. 7(a) and (b) show the beam patterns generated by our proposed method. In Fig. 7(a), we see that the MRT method achieves a maximum beamforming gain in the desired direction (i.e., the SOI), which is expected as the MRT solution is designed to match the communication channel. To better

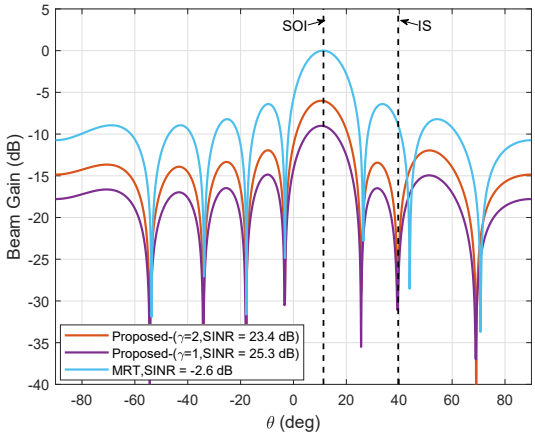

(a) Beam pattern when $K = 1$.

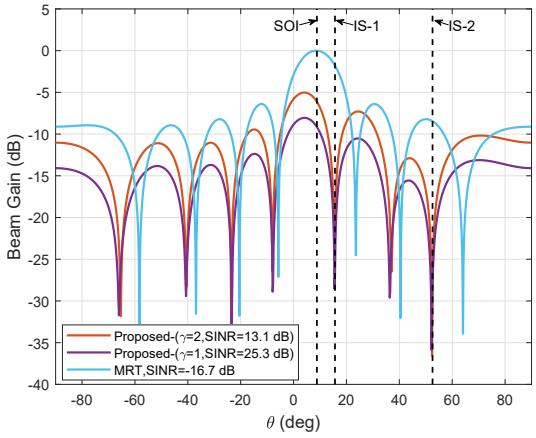

(b) Beam pattern when $K = 2$.

Fig. 7. Beam patterns at the IRS for different number of interference sources.

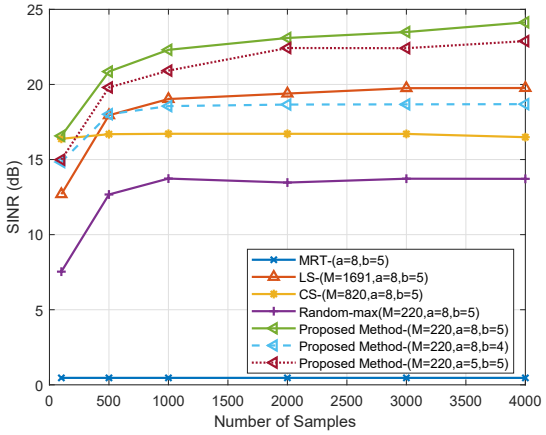

Fig. 8. SINR vs. the number of samples under different quantization bits of reflection amplitude and phase.

illustrate the performance, we normalize the beamforming gain with respect to the maximum gain achieved by the MRT solution. The MRT solution, however, is not optimized for suppressing the interference signals. As a result, the MRT method maintains a relatively high beamforming gain in the direction of the interference source (denoted as "IS"). By contrast, the proposed method may appear to "miss" the desired direction but ensures a pre-specified beamforming gain toward the SOI, meanwhile forming nulls in the directions of the interfering sources. This interference suppression results in a significant SINR improvement. Additionally, it is interesting to observe that a smaller value of γ yields a higher SINR, as it provides more degrees of freedom to suppress interference when a lower beamforming gain is required for the SOI. In Fig. 7(b), similar results are observed in the presence of two interference sources.

D. Passive IRS: Robustness Against Reflection Coefficient Discretization and Channel Uncertainty

We previously assume that the reflection coefficients can take continuous values within its specified region. In practice, due to hardware limitations, the phase shift as well as the reflection amplitude may not take arbitrary values; instead, they may have to be chosen from a finite set of discrete values. Next, we examine the robustness against the reflection coefficient discretization error. Also, we examine the robustness of the proposed method against the communication channel uncertainty.

When the reflection coefficients are constrained to discrete values, both the measurement vectors $\{\boldsymbol{a}_m\}_{m=1}^M$ and the optimized vector $\boldsymbol{a}^\star$ must adhere to this constraint. A natural approach to address this is to directly project the designed reflection coefficients onto the discretized set. Specifically, let a and b respectively represent the number of bits used to quantize the reflection amplitude and the phase shift. The discrete amplitude set $\mathcal{G}$ and the discrete phase set $\mathcal{F}$ can be expressed as:

$$\mathcal{G} = \Big\{0, \ldots, \frac{2^a - 1}{2^a}\Big\}, \mathcal{F} = \quad \Big\{0, \ldots, \frac{(2^b - 1)\pi}{2^{b-1}}\Big\}. \tag{42}$$

In Fig. 8, we illustrate the SINR achieved by respective methods as a function of the number of samples. It can be observed that the proposed method consistently outperforms the other methods by a big margin for the same level of quantization resolution. Moreover, the performance improvement becomes more significant with an increase in the quantization resolution of the phase compared to that of the amplitude. This observation reveals that the accuracy of the phase has a greater impact on the system performance.

Next, we examine the impact of inaccurate knowledge of the cascaded channel $\hat{\boldsymbol{h}}_0$ on the interference suppression

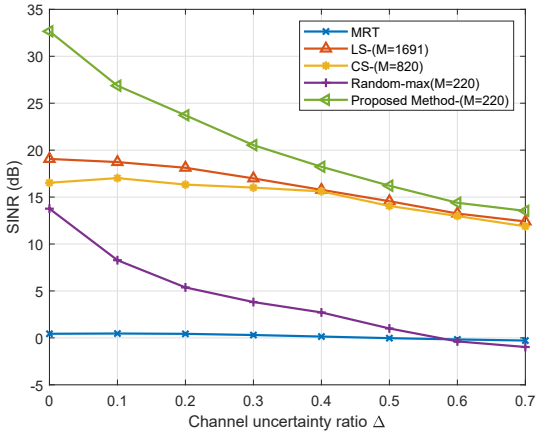

Fig. 9. SINR vs. the channel uncertainty ratio Δ.

performance. Suppose the cascaded channel $\hat{\boldsymbol{h}}_0$ is subject to a certain level of estimation errors:

$$\hat{\boldsymbol{h}}_0 = \boldsymbol{h}_0 + \Delta \times \frac{\|\boldsymbol{h}_0\|_2}{\|\boldsymbol{h}_{\text{err}}\|_2}\boldsymbol{h}_{\text{err}}, \tag{43}$$

where $\boldsymbol{h}_{\text{err}} \sim \mathcal{CN}(0, \boldsymbol{I})$ and $\Delta \in [0, 1]$ is a parameter controlling the channel uncertainty level.

Fig. 9 illustrates the SINR performance of various methods under different levels of channel uncertainty. The SINR is defined as:

$$\text{SINR}(\bar{\boldsymbol{a}}) \triangleq \frac{\|\bar{\boldsymbol{a}}^H \boldsymbol{h}_0\|_2^2}{\bar{\boldsymbol{a}}^H \boldsymbol{R}_J \bar{\boldsymbol{a}} + \sigma_w^2}, \tag{44}$$

where $\bar{\boldsymbol{a}}$ represents the optimized augmented reflection vector obtained by different methods based on the estimated cascaded channel $\hat{\boldsymbol{h}}_0$. In our simulations, the number of interference signals is set to $K = 1$, the number of samples is set to 3000, and the transmit power of the interference signal is set to 15 dB. It is observed that the performance of all methods decreases as the channel uncertainty ratio increases. The MRT method demonstrates a minimal performance loss. All other methods suffer a certain amount of performance degradation in the presence of channel inaccuracies. Nevertheless, our proposed method still achieves the highest SINR performance among all methods, while requiring substantially fewer measurements. This highlights the superiority of the proposed method over state-of-the-art methods, even with an inaccurate knowledge of $\boldsymbol{R}_0$.

VI. Conclusion

In this paper, we studied the problem of IRS-assisted ABF, where the objective is to adaptively adjust the reflection coefficients of the IRS such that the unknown interference signals at the receiver are suppressed, whereas the desired signal is well preserved. The challenge of the IRS-assisted ABF lies in that we do not have direct access to the covariance matrix. Instead, only quadratic compressive measurements of the covariance matrix are available. To address this challenge, we developed a sample-efficient method that directly solves the ABF problem relying solely on quadratic compressive measurements. Our approach demonstrated significant improvements in sample efficiency, making it highly adaptable to fast-changing wireless environments. Simulation results confirmed that the proposed method effectively cancels interference with a modest number of data samples, outperforming existing state-of-the-art algorithms.

Appendix A
Narrowband Received Signal Model

Here we focus on the received interference signal model. Without loss of generality, we consider a simplified case where only a single interference source exists. The subscript k is omitted for brevity. Let $j^{(p)}(t)$ denote the passband interference signal with a bandwidth of B_I and a carrier frequency f_I. Note that the non-cooperative interference source may use a carrier frequency that is different from that of the communication signal. The passband interference signal can be expressed as

$$j^{(p)}(t) = \Re\{\sqrt{2} j^{(b)}(t) e^{j2\pi f_I t}\}, \tag{45}$$

where $j^{(b)}(t)$ denotes the baseband interference signal [2].

Let $g^{(p)}(t)$, $p_l^{(p)}(t)$, and $q_l^{(p)}(t)$ respectively denote the passband channel between the interference source to the receiver, the interference source to the lth element of the IRS, and the lth element of the IRS to the receiver. For simplicity, here we suppose each channel contains only a line-of-sight (LOS) path:

$$g^{(p)}(t) = \alpha_g \delta(t - \tau_g), \tag{46}$$

$$p_l^{(p)}(t) = \alpha_{p,l} \delta(t - \tau_{p,l}), \tag{47}$$

$$q_l^{(p)}(t) = \alpha_{q,l} \delta(t - \tau_{q,l}), \tag{48}$$

where $\alpha_x, x \in \{\{g\}, \{p, l\}, \{q, l\}\}$ denotes the real path loss. We first consider the signal received from the direct link between the interference source and the receiver. The received passband signal can be represented by the linear convolution of the transmitted passband signal $j^{(p)}(t)$ and the channel $g^{(p)}(t)$, i.e.,

$$\begin{aligned} y_1^{(p)}(t) =& g^{(p)}(t) * j^{(p)}(t), \\ =& \alpha_g j^{(p)}(t - \tau_g), \\ =& \Re\{\alpha_g \sqrt{2} j^{(b)}(t - \tau_g) e^{j2\pi f_I (t - \tau_g)}\}, \\ =& \Re\{\alpha_g e^{-j2\pi f_I \tau_g} \sqrt{2} e^{j2\pi \Delta f t} j^{(b)}(t - \tau_g) e^{j2\pi f_c t}\} \\ =& \Re\{\sqrt{2} y_1^{(b)}(t) e^{j2\pi f_c t}\}, \end{aligned} \tag{49}$$

where $\Delta f \triangleq f_I - f_c$, and

$$y_1^{(b)}(t) = \alpha_g e^{-j2\pi f_I \tau_g} e^{j2\pi \Delta f t} j^{(b)}(t - \tau_g). \tag{50}$$

Let $Y_1^{(b)}(f)$ denote the Fourier transform of $y_1^{(b)}(t)$.

The received passband signal is then converted to a lower frequency band by multiplying the input signal with a complex sinusoid with a frequency of f_c. The down-converted signal is then filtered by a low-pass filter with a bandwith of B.

[2]We utilize subscript (p) and (b) to represent passband or baseband signals, respectively.

Let $U(f)$ denote the frequency response of an ideal low-pass filter, i.e.

$$U(f) = \begin{cases} 1 & |f| \leq B/2 \\ 0 & \text{otherwise} \end{cases}. \tag{51}$$

The received frequency-domain baseband signal can finally be written as

$$\tilde{Y}_1^{(b)}(f) = Y_1^{(b)}(f)U(f) = \alpha_g^{(b)} e^{-j2\pi f \tau_g} \tilde{J}^{(b)}(f). \tag{52}$$

where $\tilde{J}^{(b)}(f) = J^{(b)}(f - \Delta f)U(f)$, and $J^{(b)}(f)$ is the frequency response of the baseband interference signal $j^{(b)}(t)$. Here $\tilde{J}^{(b)}(f)$ can be considered as the equivalent baseband transmitted interference signal. In other words, no matter how large B_I is, the receiver can only receive a lowpass-filtered version of the interference signal.

Next, we move on to the signal received from the reflected link. Let $\theta_l^{(p)}(t)$ denote the impulse response of the lth reflecting element of the IRS. The received signal $y_2^{(p)}(t)$ from the IRS is a superposition of the received signals from all L reflecting elements, i.e.,

$$\begin{aligned} y_2^{(p)}(t) =& \sum_{l=1}^{L} p_l^{(p)}(t) * \theta_l^{(p)}(t) * q_l^{(p)}(t) * j^{(p)}(t), \\ =& \sum_{l=1}^{L} \theta_l^{(p)}(t) * \underbrace{p_l^{(p)}(t) * q_l^{(p)}(t) * j^{(p)}(t)}_{\gamma_l^{(p)}(t)}. \end{aligned} \tag{53}$$

Taking the Fourier transform of $y_2^{(p)}(t)$, we arrive at

$$Y_2^{(p)}(f) = \sum_{l=1}^{L} \Theta_l^{(p)}(f)\Gamma_l^{(p)}(f), \tag{54}$$

where $\Theta_l^{(p)}(f)$ and $\Gamma_l^{(p)}(f)$ denote the Fourier Transform of $\theta_l^{(p)}(t)$ and $\gamma_l^{(p)}(t)$, respectively.

By adopting the baseband representation $\theta_l^{(p)}(t) = \Re\{2\theta^{(b)}(t)e^{j2\pi f_c t}\}$ and $\gamma_l^{(p)}(t) = \Re\{\sqrt{2}\gamma^{(b)}(t)e^{j2\pi f_c t}\}$, the passband frequency response $\Theta_l^{(p)}(f)$ and $\Gamma_l^{(p)}(f)$ can be expressed as

$$\Theta_l^{(p)}(f) = \Theta_l^{(b)}(f - f_c) + \left(\Theta_l^{(b)}(-f - f_c)\right)^*, \tag{55}$$

$$\Gamma^{(p)}(f) = \frac{1}{\sqrt{2}}\left(\Gamma_l^{(b)}(f - f_c) + \left(\Gamma_l^{(b)}(-f - f_c)\right)^*\right), \tag{56}$$

where $()^*$ denotes the conjugate, $\Theta_l^{(b)}(f)$ and $\Gamma_l^{(b)}(f)$ denote the frequency response of $\theta_l^{(b)}(t)$ and $\gamma_l^{(b)}(t)$, respectively.

Substituting (55) and (56) into (54), we arrive at

$$\begin{aligned} Y_2^{(p)}(f) =& \frac{1}{\sqrt{2}} \sum_{l=1}^{L} \Bigg(\Theta_l^{(b)}(f - f_c)\Gamma_l^{(b)}(f - f_c) \\ &+ \left(\Theta_l^{(b)}(-f - f_c)\Gamma_l^{(b)}(-f - f_c)\right)^* \Bigg) \end{aligned} \tag{57}$$

It is observed that $Y_2^{(p)}(f)$ has a form similar to (56). As a result, the baseband frequency response $Y_2^{(b)}(f)$ after down-shifting and low-pass filtering is given as

$$Y_2^{(b)}(f) = \sum_{l=1}^{L} \Theta_l^{(b)}(f)\Gamma_l^{(b)}(f)U(f), \tag{58}$$

where $U(f)$ is defined in (51). By reformulating (55), we have

$$\Theta_l^{(b)}(f)U(f) = \Theta_l^{(p)}(f + f_c)U(f), \tag{59}$$

According to the transmission line theory, the frequency response $\Theta_l^{(p)}(f)$ can be characterized by

$$\Theta_l^{(p)}(f) = \frac{Z_l(f) - Z_0}{Z_l(f) + Z_0}, \tag{60}$$

where $Z_l(f)$ denotes the reconfigurable impedance of the lth reflecting element, which is dependent on the frequency, and Z_0 denotes the free space impedance. Generally, the frequency response of the IRS varies as the frequency changes. Nevertheless, the response of the IRS is specially designed around the communication carrier frequency f_c. If the communication signal bandwidth B is limited by a few tens of MHz, the phase varies approximately linearly with the frequency and the amplitude response remains nearly constant as compared to the large path loss induced by wireless channels [7]. Hence, the baseband frequency response $\Theta_l^{(b)}(f)$ can be simplified as

$$\Theta_l^{(b)}(f) \approx \beta_l e^{-j2\pi f_c \tau_l} e^{-j2\pi f \tau_l}, \quad |f| \leq B/2. \tag{61}$$

where τ_l denotes the delay introduced by the corresponding reflecting element. As a result, the baseband impulse response of the lth reflecting element of IRS can be simplified as

$$\theta_l^{(b)}(t) = \beta_l e^{-j2\pi f_c \tau_l} \delta(t - \tau_l). \tag{62}$$

Now, let us come back to the received signal in (53). By substituting (45), (47), (48), and (62) into (53), we have

$$\begin{aligned} y_2^{(p)}(t) =& \sum_{l=1}^{L} p_l^{(p)}(t) * \theta_l^{(p)}(t) * q_l^{(p)}(t) * j^{(p)}(t), \\ =& \sum_{l=1}^{L} \alpha_{p,l}\alpha_{q,l}\beta_l j^{(p)}(t - \tau_{p,l} - \tau_{q,l} - \tau_l), \\ =& \Re\Big\{ \sum_{l=1}^{L} \alpha_{p,l}^{(b)}\alpha_{q,l}^{(b)}\beta_l^{(b)}\sqrt{2}e^{j2\pi\Delta f(t-\tilde{\tau}_l)} j^{(b)}(t - \tilde{\tau}_l)e^{j2\pi f_c t}\Big\}, \\ =& \Re\big\{\sqrt{2}y_2^{(b)}(t)e^{j2\pi f_c t}\big\} \end{aligned} \tag{63}$$

where

$$\begin{aligned} \alpha_{p,l}^{(b)} =& \alpha_{p,l}e^{-j2\pi f_c \tau_{p,l}}, \quad \alpha_{q,l}^{(b)} = \alpha_{q,l}e^{-j2\pi f_c \tau_{q,l}}, \\ \beta_l^{(b)} =& \beta_l e^{-j2\pi f_c \tau_l}, \quad \tilde{\tau}_l = \tau_{p,l} + \tau_{q,l} + \tau_l. \end{aligned} \tag{64}$$

Thus, the frequency response of the equivalent baseband received signal is given by

$$Y_2^{(b)}(f) = \alpha_{p,l}^{(b)}\alpha_{q,l}^{(b)}\beta_l^{(b)} e^{-j2\pi f \tilde{\tau}_l} \tilde{J}^{(b)}(f). \tag{65}$$

where $\tilde{J}^{(b)}(f)$ is defined in (52). Combining (52) and (65), the received equivalent baseband signal at the receiver is the summation of signals from the direct link and reflected link, i.e.,

$$\begin{aligned} Y^{(b)}(f) =& Y_2^{(b)}(f) + Y_1^{(b)}(f) = \Bigg(\sum_{l=1}^{M} \alpha_{p,l}^{(b)}\alpha_{q,l}^{(b)}\beta_l^{(b)} e^{-j2\pi f \tilde{\tau}_l} \\ &+ \alpha_g^{(b)} e^{-j2\pi f \tau_g} \Bigg) \tilde{J}^{(b)}(f), \quad |f| \leq \frac{B}{2} \end{aligned} \tag{66}$$

If the two phase terms $e^{-j2\pi f\tilde{\tau}_l}$ and $e^{-j2\pi f\tau_g}$ are nearly the same for all frequencies $|f| \leq B/2$, it means that the received baseband signals from the direct link and the reflected link are the same, except for being scaled by different factors. Hence by adjusting the reflecting coefficients $\{\beta_l^{(b)}\}$, it is possible to nullify the interference signal at the baseband of the receiver.

Let $\tilde{\tau}_l^\star = (\tau_{p,l}^\star + \tau_{q,l}^\star + \tau_l^\star)$ denote the maximum delay introduced by the reflecting element. To ensure $e^{-j2\pi f\tilde{\tau}_l}$ and $e^{-j2\pi f\tau_g}$ are nearly the same for all frequencies $|f| \leq B/2$, it is sufficient to let

$$\frac{e^{-j2\pi f\tilde{\tau}_l^\star}}{e^{-j2\pi f\tau_g}} \to 1, \forall |f| \leq \frac{B}{2} \tag{67}$$

which is equivalent to

$$B(\tau_{p,l}^\star + \tau_{q,l}^\star + \tau_l^\star - \tau_g) \ll 1 \tag{68}$$

Also, since the reflecting element of the IRS introduces a much smaller delay than delays caused by wireless propagation channels, the above condition can be further simplified as

$$B(\tau_{p,l}^\star + \tau_{q,l}^\star - \tau_g) = B\delta_\tau \ll 1. \tag{69}$$

As a result, (66) can be further simplified as

$$Y^{(b)}(f) = \left(\sum_{l=1}^{L} \alpha_{p,l}^{(b)}\alpha_{q,l}^{(b)}\beta_l^{(b)} + \alpha_g^{(b)}\right) e^{-j2\pi f\tau_g}\tilde{J}^{(b)}(f), \tag{70}$$

where $e^{-j2\pi f\tau_g} \approx e^{-j2\pi f\tilde{\tau}_l}, \forall |f| \leq B/2$. Accordingly, the equivalent baseband received signal model after time synchronisation and sampling at the tth time instant can be expressed as

$$y(t) = \alpha_g^{(b)} j(t) + \sum_{l=1}^{L} \alpha_{p,l}^{(b)}\alpha_{q,l}^{(b)}\beta_l^{(b)} j(t) + \epsilon(t), \tag{71}$$

Let $\boldsymbol{\Theta} = \mathrm{diag}(\beta_1^{(b)}, \ldots, \beta_L^{(b)})$ denote the reflection coefficient matrix of the IRS, $g = \alpha_g^{(b)}$ denote the direct channel between the interference source and the receiver, $\boldsymbol{q}^H = [\alpha_{q,1}^{(b)}, \ldots, \alpha_{q,L}^{(b)}]^T \in \mathbb{C}^L$ and $\boldsymbol{p}^H = [\alpha_{p,1}^{(b)}, \ldots, \alpha_{p,L}^{(b)}]^T \in \mathbb{C}^L$, the received signal in (71) can be written in a more compact form

$$y(t) = (g + \boldsymbol{q}^H\boldsymbol{\Theta}\boldsymbol{p})j(t) + \epsilon(t), \tag{72}$$

When the legitimate transmitter sends a communication signal $s(t)$, the overall received signal at the receiver can be represented by (1).

REFERENCES

[1] Q. Wu and R. Zhang, "Intelligent Reflecting Surface Enhanced Wireless Network via Joint Active and Passive Beamforming," *IEEE Trans. Wireless Commun.*, vol. 18, no. 11, pp. 5394–5409, 2019.

[2] C. Huang, A. Zappone, G. C. Alexandropoulos, M. Debbah, and C. Yuen, "Reconfigurable Intelligent Surfaces for Energy Efficiency in Wireless Communication," *IEEE Trans. Wireless Commun.*, vol. 18, no. 8, pp. 4157–4170, 2019.

[3] Q. Wu and R. Zhang, "Towards Smart and Reconfigurable Environment: Intelligent Reflecting Surface Aided Wireless Network," *IEEE Commun. Mag.*, vol. 58, no. 1, pp. 106–112, Jan. 2020.

[4] R. Long, Y.-C. Liang, Y. Pei, and E. G. Larsson, "Active reconfigurable intelligent surface-aided wireless communications," *IEEE Trans. Wireless Commun.*, vol. 20, no. 8, pp. 4962–4975, 2021.

[5] C. Pan *et al.*, "An overview of signal processing techniques for RIS/IRS-aided wireless systems," *IEEE J. Sel. Topics Signal Process.*, vol. 16, no. 5, pp. 883–917, Aug. 2022.

[6] P. Wang, W. Mei, J. Fang, and R. Zhang, "Target-Mounted Intelligent Reflecting Surface for Joint Location and Orientation Estimation," *IEEE J. Select. Areas Commun.*, vol. 41, no. 12, pp. 3768–3782, Dec. 2023.

[7] E. Björnson, H. Wymeersch, B. Matthiesen, P. Popovski, L. Sanguinetti, and E. de Carvalho, "Reconfigurable intelligent surfaces: A signal processing perspective with wireless applications," *IEEE Signal Process. Mag.*, vol. 39, no. 2, pp. 135–158, 2022.

[8] T. J. Cui, M. Q. Qi, X. Wan, J. Zhao, and Q. Cheng, "Coding metamaterials, digital metamaterials and programmable metamaterials," *Light Sci Appl*, vol. 3, no. 10, pp. e218–e218, Oct. 2014.

[9] P. Wang, J. Fang, X. Yuan, Z. Chen, and H. Li, "Intelligent Reflecting Surface-Assisted Millimeter Wave Communications: Joint Active and Passive Precoding Design," *IEEE Trans. Veh. Technol.*, vol. 69, no. 12, pp. 14 960–14 973, Dec. 2020.

[10] P. Wang, J. Fang, L. Dai, and H. Li, "Joint Transceiver and Large Intelligent Surface Design for Massive MIMO mmWave Systems," *IEEE Trans. Wireless Commun.*, vol. 20, no. 2, pp. 1052–1064, Feb. 2021.

[11] J. Chen, Y.-C. Liang, Y. Pei, and H. Guo, "Intelligent Reflecting Surface: A Programmable Wireless Environment for Physical Layer Security," *IEEE Access*, vol. 7, pp. 82 599–82 612, 2019.

[12] S. Xu, J. Liu, and Y. Cao, "Intelligent reflecting surface empowered physical-layer security: Signal cancellation or jamming?" *IEEE Internet Things. J.*, vol. 9, no. 2, pp. 1265–1275, 2021.

[13] D. Mishra and H. Johansson, "Channel estimation and low-complexity beamforming design for passive intelligent surface assisted miso wireless energy transfer," in *Proc. IEEE Int. Conf. Acoustics, Speech. Signal Process.*, 2019, pp. 4659–4663.

[14] P. Wang, J. Fang, H. Duan, and H. Li, "Compressed channel estimation for intelligent reflecting surface-assisted millimeter wave systems," *IEEE Signal Process. Lett.*, vol. 27, pp. 905–909, May 2020.

[15] T. L. Jensen and E. De Carvalho, "An optimal channel estimation scheme for intelligent reflecting surfaces based on a minimum variance unbiased estimator," in *Proc. IEEE Int. Conf. Acoustics, Speech. Signal Process.*, May 2020, pp. 5000–5004.

[16] P. Wang, J. Fang, W. Zhang, and H. Li, "Fast beam training and alignment for IRS-assisted millimeter wave/terahertz systems," *IEEE Trans. Wireless Commun.*, vol. 21, no. 4, pp. 2710–2724, Apr. 2022.

[17] B. Zheng, C. You, W. Mei, and R. Zhang, "A survey on channel estimation and practical passive beamforming design for intelligent reflecting surface aided wireless communications," *IEEE Commun. Surveys Tuts.*, vol. 24, no. 2, pp. 1035–1071, 2022.

[18] F. Wang, H. Li, and A. L. Swindlehurst, "Clutter suppression for target detection using hybrid reconfigurable intelligent surfaces," in *Proc. IEEE Radar Conf. (RadarConf23)*, San Antonio, TX, USA, 01-05 May 2023, pp. 1–5.

[19] V. Arun and H. Balakrishnan, "RFocus: Beamforming Using Thousands of Passive Antennas," in *Proc. USENIX Symp. Netw. Syst. Des. Implementation (NSDI)*. Santa Clara, CA: USENIX Association, Feb. 2020, pp. 1047–1061.

[20] S. Ren, K. Shen, Y. Zhang, X. Li, X. Chen, and Z.-Q. Luo, "Configuring Intelligent Reflecting Surface With Performance Guarantees: Blind Beamforming," *IEEE Trans. Wireless Commun.*, vol. 22, no. 5, pp. 3355–3370, May 2023.

[21] F. Xu, J. Yao, W. Lai, K. Shen, X. Li, X. Chen, and Z.-Q. Luo, "Coordinating multiple intelligent reflecting surfaces without channel information," *IEEE Trans. Signal Process.*, vol. 72, pp. 31–46, 2023.

[22] W. Lai, W. Wang, F. Xu, X. Li, S. Niu, and K. Shen, "Blind Beamforming for Intelligent Reflecting Surface in Fading Channels without CSI," *arXiv preprint arXiv:2305.18998*, 2023.

[23] W. Lai and K. Shen, "Blind Beamforming for Intelligent Reflecting Surface: A Reinforcement Learning Approach," in *Proc. IEEE Int. Conf. Acoustics, Speech. Signal Process.* Seoul, Korea, Republic of: IEEE, Apr. 2024, pp. 8956–8960.

[24] Yuxin Chen, Yuejie Chi, and A. J. Goldsmith, "Exact and Stable Covariance Estimation From Quadratic Sampling via Convex Programming," *IEEE Trans. Inform. Theory*, vol. 61, no. 7, pp. 4034–4059, July 2015.

[25] Y. Chi, "Kronecker covariance sketching for spatial-temporal data," in *Proc. European Signal Process. Conf. (EUSIPCO)*, 2016, pp. 316–320.

[26] Y. Li, C. Ma, Y. Chen, and Y. Chi, "Nonconvex Matrix Factorization From Rank-One Measurements," *IEEE Trans. Inform. Theory*, vol. 67, no. 3, pp. 1928–1950, Mar. 2021.

[27] J. Liao, S. Guo, L. Yuan, C. Ji, C. Huang, and X. Luo, "Independent manipulation of reflection amplitude and phase by a single-layer reconfigurable metasurface," *Advanced Optical Materials*, vol. 10, no. 4, p. 2101551, 2022.
[28] Q. Yan, H. Zeng, T. Jiang, M. Li, W. Lou, and Y. T. Hou, "Jamming Resilient Communication Using MIMO Interference Cancellation," *IEEE Trans. Information Forensics Secur.*, vol. 11, no. 7, pp. 1486–1499, 2016.
[29] M. Grant and S. Boyd, "CVX: Matlab software for disciplined convex programming, version 2.1," https://cvxr.com/cvx, Mar. 2014.
[30] J. Miranda, R. Abrishambaf, T. Gomes, P. Gonçalves, J. Cabral, A. Tavares, and J. Monteiro, "Path loss exponent analysis in wireless sensor networks: Experimental evaluation," in *Proc. IEEE Int. Conf. Ind. Inform. (INDIN)*, 2013, pp. 54–58.

Peilan Wang (Memeber, IEEE) received the B.Eng. and the Ph.D. degree from the University of Electronic Science and Technology (UESTC), Chengdu, China, in 2018 and 2023, respectively. From 2022 to 2023, she was a Visiting Research Scholar with the Department of Electrical and Computer Engineering, National University of Singapore (NUS). She is now working as a Postdoctoral Research Associate with the National Key Laboratory of Wireless Communications, UESTC. Her current research interests include compressed sensing, millimeter wave/THz communications, intelligent reflecting surface, signal processing, and integrated sensing and communications.

Jun Fang (SM'19) received the B.S. and M.S. degrees from the Xidian University, Xi'an, China in 1998 and 2001, respectively, and the Ph.D. degree from the National University of Singapore, Singapore, in 2006, all in electrical engineering.

During 2006, he was a postdoctoral research associate in the Department of Electrical and Computer Engineering, Duke University. From January 2007 to December 2010, he was a research associate with the Department of Electrical and Computer Engineering, Stevens Institute of Technology. Since 2011, he has been with the University of Electronic of Science and Technology of China, where he is currently a Professor. His research interests include compressed sensing and sparse theory, massive MIMO/mmWave communications, and statistical inference.

Dr. Fang was the recipient of the IEEE Jack Neubauer Memorial Award in 2013 for the best systems paper published in the *IEEE Transactions on Vehicular Technology*, and the recipient of the 2024 IEEE Signal Processing Letters Best Paper Award. He served as an Associate Technical Editor for *IEEE Communications Magazine* from 2012 to 2020, and a Senior Associate Editor for *IEEE Signal Processing Letters* from 2018 to 2022. He is currently a Member of the IEEE SPS Sensor Array and Multichannel TC.

Bin Wang (S'16-M'21) received the Ph.D. degree in Electrical Engineering from the University of Electronic of Science and Technology of China (UESTC) in 2021. He is now working as a postdoctoral research associate in the National Key Laboratory of Wireless Communications, UESTC. His research interests include stochastic optimization, wireless communications and machine learning.

Hongbin Li (M'99-SM'08-F'19) received the B.S. and M.S. degrees from the University of Electronic Science and Technology of China, in 1991 and 1994, respectively, and the Ph.D. degree from the University of Florida, Gainesville, FL, in 1999, all in electrical engineering.

From July 1996 to May 1999, he was a Research Assistant in the Department of Electrical and Computer Engineering at the University of Florida. Since July 1999, he has been with the Department of Electrical and Computer Engineering, Stevens Institute of Technology, Hoboken, NJ, where he is currently the Charles and Rosanna Batchelor Memorial Chair Professor. He was a Summer Visiting Faculty Member at the Air Force Research Laboratory in the summers of 2003, 2004 and 2009. His general research interests include statistical signal processing, wireless communications, and radars.

Dr. Li received a number of awards including the IEEE Jack Neubauer Memorial Award in 2013, Master of Engineering (Honoris Causa) from Stevens Institute of Technology in 2024, Provost's Award for Research Excellence in 2019, Harvey N. Davis Teaching Award in 2003, and Jess H. Davis Memorial Research Award in 2001, and Sigma Xi Graduate Research Award in 1999. He has been a member of the IEEE SPS Signal Processing Theory and Methods Technical Committee (TC) and the IEEE SPS Sensor Array and Multichannel TC, an Associate Editor for *Signal Processing* (Elsevier), *IEEE Transactions on Signal Processing*, *IEEE Signal Processing Letters*, and *IEEE Transactions on Wireless Communications*, as well as a Guest Editor for *IEEE Journal of Selected Topics in Signal Processing* and *EURASIP Journal on Applied Signal Processing*. He has been involved in various conference organization activities, including serving as a General Co-Chair for the 7th IEEE Sensor Array and Multichannel Signal Processing (SAM) Workshop, Hoboken, NJ, June 17-20, 2012. Dr. Li is a member of Tau Beta Pi and Phi Kappa Phi, and a fellow of the Asia-Pacific Artificial Intelligence Association (AAIA) and the International Artificial Intelligence Industry Alliance (AIIA).